

Calibration and Validation of an HMA Fracture Mechanics Based Enhanced Cracking Performance Model

Jian Zou¹⁺ and Reynaldo Roque¹

Abstract: An HMA fracture mechanics based enhanced cracking performance model (HMA-FM-E) was calibrated and validated using selected Florida field sections. The model calibration was undertaken by matching as closely as possible predicted top-down cracking performance with field observations. Also, predictions using the calibrated model showed that the predicted crack growth rates and crack initiation times were inversely-related, which is reasonable and agrees with our field experience. The model validation effort using the prediction sum of squares approach demonstrated the strong predictability of the calibrated model. Further calibration of the model is recommended when more field sections with high quality data are available. Also, further development and integration of submodels such as the predictive relationship for initial fracture energy based on gradation characterization and volumetric properties can be employed to make the HMA-FM-E a Level-3 design tool suitable for use in the mechanistic-empirical pavement design.

DOI:10.6135/ijprt.org.tw/2014.7(2).93

Key words: Aging; Fracture and damage properties; HMA fracture mechanics; Pavement design; Pavement performance model.

Introduction

Top-down cracking, which initiates at the surface of the pavement and propagates downward through the HMA layer, is now commonly recognized as a major form of distress that reduces the service life of asphalt pavements [1-4]. Experimental methods that may provide the properties necessary to evaluate the susceptibility of HMA mixtures to this type of distress have been proposed by some researchers [5-6]. Hypotheses regarding the mechanisms of top-down cracking have also been developed [7-8]. Recently, a hot mix asphalt fracture mechanics (HMA-FM) model that predicts crack growth in a stepwise manner was developed [9-10]. The HMA-FM model accounts for the combined effects of damage and fracture related properties on fracture performance of asphalt mixture. Based on the HMA-FM model, an enhanced model was further developed for predicting top-down cracking performance in asphalt pavements [11-12]. The HMA-FM-Based enhanced cracking performance model (HMA-FM-E) is capable of predicting the entire process of top-down cracking from the onset of cracking to pavement failure, which provides valuable information for material and pavement engineers to optimize their designs and potentially helps mitigate this type of distress. This study mainly presents the efforts for calibration and validation of the enhanced cracking performance model. A brief introduction of the HMA-FM-E, including the theoretical basis and major components of the enhanced model, is provided below.

The HMA-FM model was motivated by the fact that asphalt mixture has a fundamental dissipated creep strain energy limit (fracture threshold), which has been determined to be independent

of loading mode and history. Cracking will initiate or propagate in any region of the asphalt mixture where induced damage exceeds the threshold. As a result, the model predicts crack growth in a stepwise manner that is more practical than the continuous manner driven by the Paris Law employed in many traditional fatigue models. Fig. 1 illustrates the basic principle of the HMA-FM using two mixtures with different properties. For either mixture, the induced damage in terms of dissipated creep strain energy (DCSE) increases with number of load repetitions (N). Mixture 1 with a higher creep rate exhibits a higher rate of damage accumulation than Mixture 2. However, it does not necessarily imply that Mixture 2 will have better fracture performance, because fracture performance of mixture is also dependent on DCSE limit (fracture threshold), which is not necessarily related to the creep characteristics of the mixture. As shown in the figure, Mixture 2 will crack before Mixture 1 if it has a low threshold ($DCSE_{f2B}$), or it will crack after Mixture 1 if it has a higher threshold ($DCSE_{f2A}$). The example illustrates that the HMA-FM model is able to evaluate fracture performance of asphalt mixture by accounting for multiple key mixture properties that are known to control cracking performance. Also, it demonstrated that no single mixture property can be used to reliably predict fracture performance of asphalt mixture.

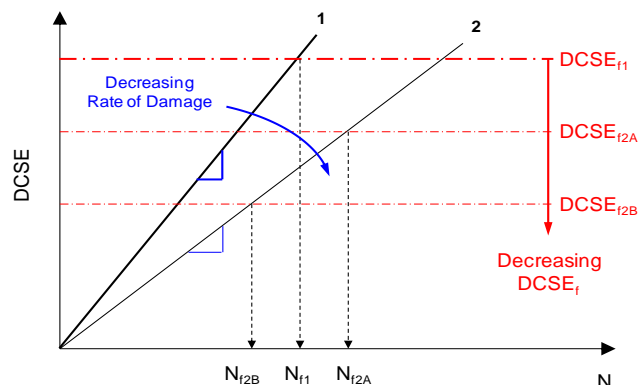


Fig. 1. Illustration of Basic Principles of the HMA-FM.

¹ Department of Civil and Coastal Engineering, University of Florida, 365 Weil Hall PO Box 116580, Gainesville, FL 32611, USA.

⁺ Corresponding Author: E-mail zouj@ufl.edu

Note: Submitted January 31, 2013; Revised September 24, 2013; Accepted September 26, 2013.

The HMA-FM-E maintained the aforementioned fundamental elements of the HMA-FM system. Major enhancements included the development and introduction of sub-models that account for two key factors: aging and healing, which were shown to have significant influence on top-down cracking performance [13]. As shown in the general model framework presented in Fig. 2, the HMA-FM-E has four major components: (i) the mixture property sub-models to account for changes of damage, fracture, and healing properties of the mixture due to oxidative aging, (ii) the load response and load-associated damage sub-models to predict load induced damage, (iii) the thermal response and thermal-associated damage sub-models to predict thermally induced damage, and (iv) the damage recovery and accumulation process to accumulate damage after taking healing effects into account. Once the accumulated damage reaches an energy-based threshold, a crack will initiate or propagate. The main mechanisms considered in the model included the load-induced factor (mode-I-tension), the temperature-induced factor (thermal stress), and material factors (damage, fracture, and healing properties and their changes as affected by aging). Details for these mechanisms and major components are described elsewhere [11-12].

In this study, the HMA-FM-E will be calibrated following a two-stage process: Stage I, selecting field sections, and collecting and analysing data related to field performance and material properties. The field performance data will be used to determine crack initiation times of all field sections, and the material property data are needed in conducting performance prediction with the enhanced model. Stage II, undertaking model prediction and determining calibration factor(s) of the model by matching as closely as possible top-down cracking predictions with observed cracking performance in the field. Then, the predictability of the enhanced model will be assessed using the prediction sum of squares (PRESS) approach.

Objectives

The primary objective of this study was to calibrate and validate the HMA-FM-Based enhanced cracking performance model to determine whether the enhanced model could reasonably predict top-down cracking performance of asphalt concrete pavement for different pavement structures, mixture properties, and traffic levels. Detailed objectives are summarized as follows:

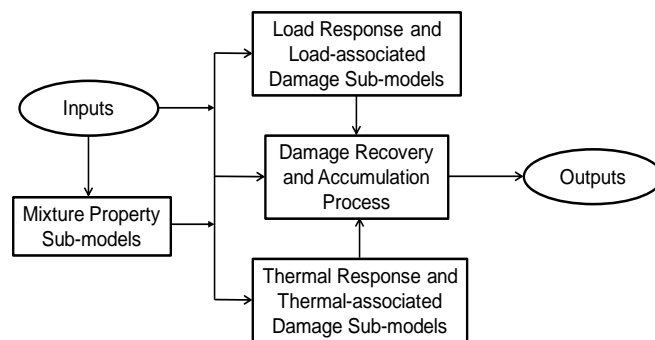


Fig. 2. General Framework of the HMA-FM-E.

- Present the effort of collecting cracking performance data from selected field sections and conducting laboratory testing on field cores, and conduct data analysis to facilitate model calibration and validation
- Undertake model prediction for these field sections using the HMA-FM-E and determine calibration factor(s) by matching as closely as possible predicted and observed cracking performance
- Assess the predictability of the calibrated performance model using the PRESS approach

Field Evaluation and Laboratory Testing

Ten Florida field sections were carefully selected for the calibration and validation efforts of this work. Only sections that satisfy the following two criteria were used: (i) pavement performance data were determined through a comparison of pavement condition survey data and direct field observations, and (ii) material property data were obtained from Superpave indirect tensile (IDT) tests performed on field cores. Table 1 summarizes the selected field pavements which are composed of interstate highways and state roads covering a broad range of structures and traffic levels.

Field Evaluation

Field evaluation was conducted to determine the cracking performance of all ten field sections, including analysis of cracking rating data and results of visual inspection of field sections.

Crack rating data is part of the data collected and maintained by

Table 1. Field Sections Selected for the Calibration and Validation Efforts.

Section ID	Section Name	County	Road Type	Traffic/Year (KESALs) ^a
1	I-75 S1A	Charlotte	Interstate Highway	573
2	I-75 S1B	Charlotte	Interstate Highway	558
3	I-75 S3	Lee	Interstate Highway	674
4	I-75 S2	Lee	Interstate Highway	576
6	SR-80 S2	Lee	State Road	207
7	I-10 S1A	Suwannee	Interstate Highway	392
8	I-10 S1B	Suwannee	Interstate Highway	392
9	SR-471	Sumter	State Road	26
10	SR-19	Lake	State Road	51
11	SR-997	Dade	State Road	89

^a “KESALs” denotes thousand ESALs.

Table 2. Cracking State and Crack Initiation Time for Field Sections.

Section ID	Age (year)	PCS-based		Observed	Final Decision	
		State	t_i (year)	State	State	t_i (year)
1	15	C	10	C	C	10
2	14	C	12	U	C*	12
3	15	C	11	C	C	11
4	14	U	17 (P)	U	U	17 (P)
6	19	U	22 (P)	U	U	22 (P)
7	7	U	8 (P)	C	C*	< 7
8	7	U	8 (P)	U	U	8 (P)
9	3	C	2	C	C	2
10	3	C	1	C	C	1
11	40	C	38	U	C*	38

Note: “C” denotes cracked state; “U” denotes uncracked state; “P” indicates that the value was determined based on linear extrapolation; “*” denotes the final decision.

the Florida Department of Transportation (FDOT) during their annually conducted pavement condition survey (PCS). It provides a detailed summary of pavement condition that can be used to assist in the determination of major maintenance or rehabilitation work. In the PCS system, a crack rating which measures percent area affected by the cracking is reported on a 0 to 10 scale with 10 as the best condition. A reduction in crack rating means that cracks occurred either confined to wheel paths (CW) or outside of wheel paths (CO) or both [14]. In this part of the study, the historical crack rating data for each of the pavements acquired from the FDOT were carefully examined to preliminarily determine pavement cracking state and estimate crack initiation time. A summary of these results determined for each pavement section is shown in the “PCS-based” columns of Table 2. For example, Section 2 was cracked at the age of 14 years and its crack initiation time was determined to be 12 years. Section 4 was uncracked at the age of 14 years and its crack initiation time was estimated to be 17 years based on extrapolation of the crack rating data. Fig. 3 illustrates the approach used to estimate the onset of cracking, where a critical crack rating of 8.0 was selected as the threshold [11].

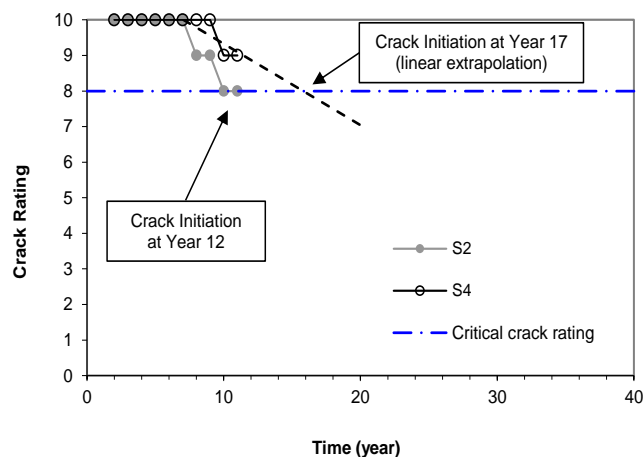


Fig. 3. Estimation of Crack Initiation Time Based on Crack Rating (Sections 2 and 4).

possibly due to poor weather/light conditions.

Laboratory Testing on Field Cores

An independent visual inspection of all pavement sections was conducted by the research team at the University of Florida (UF) in 2003 to obtain information of pavement condition and identify specific distress patterns [15]. Based on the results of field inspection, a plan regarding locations for sampling (coring) was determined and then cores were taken and brought to the UF laboratory for testing. The observed field cracking performance is summarized as: (i) uncracked pavement sections (Sections 2, 4, 6, 8, and 11) generally exhibited good condition and had no cracks, and (ii) longitudinal cracks were observed in cracked pavement sections (Sections 1, 3, 7, 9, and 10).

Superpave IDT tests were used to determine mixture properties on cut cores, including fracture energy limit, creep rate, and resilient modulus [15]. Fracture energy limit is the total energy necessary to induce fracture. It represents the tolerance of the mixture to fracture. Creep rate is the rate of the creep compliance curve at 1000-second loading time, which has been shown in prior work to be related to the rate of damage accumulation of the mixture [9]. Resilient modulus was defined as the ratio of the applied stress to recoverable strain when repeated loads were applied. It represents the elastic stiffness of asphalt mixture. Three replicates are required for each set of the IDT tests. Details on testing and data analysis procedures to calculate these parameters are described elsewhere [16]. Fig. 4 presents these mixture properties determined on field cores taken from different pavement sections. It appeared that all four young sections (i.e., Sections 7 to 10) had poor cracking performance, as indicated by crack initiation times of less than 10 years. Among these sections, 7 and 8 (Fig. 4(a)) had relatively low fracture energy limits after being in service for only seven years, while Section 9

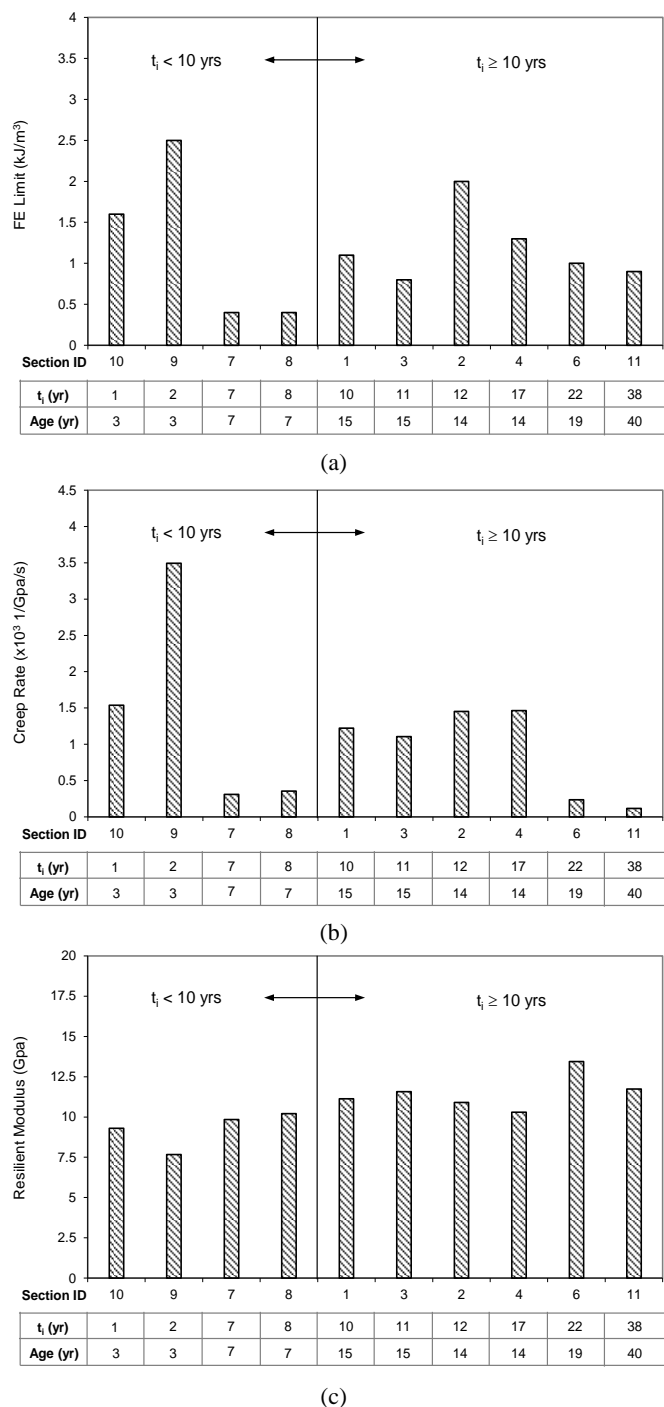


Fig. 4. Mixture Properties Determined on Cores from Different Pavement Sections: (a) FE Limit, (b) Creep Rate, and (c) Resilient Modulus.

(Fig. 4(b)) exhibited a relatively high creep rate. Also, it can be seen that mixture stiffness of those younger sections was generally lower than the others (Fig. 4(c)).

Model Calibration

There is only one parameter, i.e., the aging parameter k_1 that needs to be calibrated in the top-down cracking performance model [11]. The others can be obtained from various sources as described in

Subsection 3.1. Model calibration was conducted to determine the aging parameter k_1 by matching as closely as possible predicted with observed top-down cracking performance in the field, i.e., crack initiation time in this study.

Data Required by the Performance Model

The input data required by the HMA-FM-E was divided into five categories, i.e., pavement structure, moduli of unbound materials and asphalt concrete (AC), fracture and healing property of AC, temperature of AC, and traffic. Details regarding input data for each category are described as follows.

- **Structural property:** A four-layer pavement structure was selected for the simulation (see Table 3(a)). Thicknesses for AC, unbound base and subbase were obtained from design values.
- **Modulus of unbound materials:** Base, subbase and subgrade moduli were determined based on back-analysis of data from falling weight deflectometer (FWD) test conducted at the time of field evaluation (see Table 3(a)). The changes in Base and Subgrade moduli over time were not considered because the former is negligible in Florida because of the low permeability of bases, and the latter has a small effect on top-down cracking.
- **Modulus of AC:** The variation of AC modulus due to aging was predicted using the AC stiffness aging sub-model which requires gradation, binder type, and volumetric properties as provided in Table 3(b), where V_{beff} is effective binder content (percent by volume), V_a is percent air void, and MAAT denotes mean annual air temperature.
- **AC fracture and healing property:** Variations of AC fracture property and healing potential over time/age were predicted using the FE limit aging sub-model and the healing sub-model. These two submodels require measured properties on field cores using the IDT tests, as shown in Fig. 4, where creep rate was determined based on creep compliance master curve [17].
- **AC temperature:** A non-freeze climate in Melrose, FL was selected for this simulation. Based on the climatic condition and typical pavement material and structural properties of this area, hourly temperature variation at different depths in the AC layer was obtained using the enhanced integrated climatic model [18]. The difference in AC temperature across different project locations in Florida was ignored because the temperature effect on top-down cracking was shown to be negligible based on a sensitivity analysis conducted in a separate study [12].
- **Traffic:** The traffic data obtained for the year of field evaluation was used in the simulation (see Table 3(a)).

Determination of Aging Parameter k_1

The aging parameter k_1 is one of the key parameters defining the predictive relationship for fracture energy limit FE_f shown in Eq. (1), where t is age (in year), FE_i is the initial fracture energy of the AC, FE_{min} is the minimum value of the FE after a sufficiently long aging period t_f , and $S_n(t)$ is the normalized change in stiffness at the surface of the AC layer. In this study, FE_{min} was determined to be

Table 3. Data Used for Model Prediction in all Ten Sections.

(a) Pavement Structural and Material Property and Traffic

Section ID	Layer Thickness (cm)			Layer Modulus (MPa)			Traffic/Year (KESALs)
	AC	Base	Subbase	Base	Subbase	Subgrade	
1	16.6	30.5	30.5	377.6	345.5	207.8	573
2	15.8	30.5	30.5	438.5	354.4	248.8	558
3	16.5	30.5	30.5	411.1	240.0	249.8	674
4	18.8	30.5	30.5	740.1	622.8	216.2	576
6	16.0	30.5	30.5	394.9	314.1	129.7	207
7	18.3	30.5	30.5	384.2	375.9	268.0	392
8	18.8	30.5	30.5	449.3	285.5	321.3	392
9	6.6	30.5	30.5	296.4	234.4	231.6	26
10	6.1	30.5	30.5	349.5	89.6	86.9	51
11	5.5	30.5	30.5	751.4	365.4	363.3	89

(b) Mixture Gradation and Volumetric Property

Section ID	Percent Passing by Weight				V _{beff} (%)	V _a (%)	MAAT (°C)	Binder Type
	19 (mm)	9.5 (mm)	4.75 (mm)	0.075 (mm)				
1	100.0	91.8	73.6	5.9	10.7	5.4	23.9	PG67-22
2	100.0	93.7	74.6	5.6	10.7	3.2	23.9	PG67-22
3	100.0	86.2	65.1	5.5	8.2	7.2	23.9	PG67-22
4	100.0	92.5	68.9	5.0	8.4	6.9	23.9	PG67-22
6	100.0	84.8	64.4	6.2	8.9	7.5	23.9	PG67-22
7	100.0	90.0	60.2	4.8	10.3	8.7	23.9	PG67-22
8	100.0	90.0	60.2	4.8	9.1	9.9	23.9	PG67-22
9	100.0	90.0	60.2	4.8	13.3	5.7	23.9	PG67-22
10	100.0	90.0	60.2	4.8	14.2	4.8	23.9	PG67-22
11	100.0	90.0	60.2	4.8	11.4	7.6	23.9	PG67-22

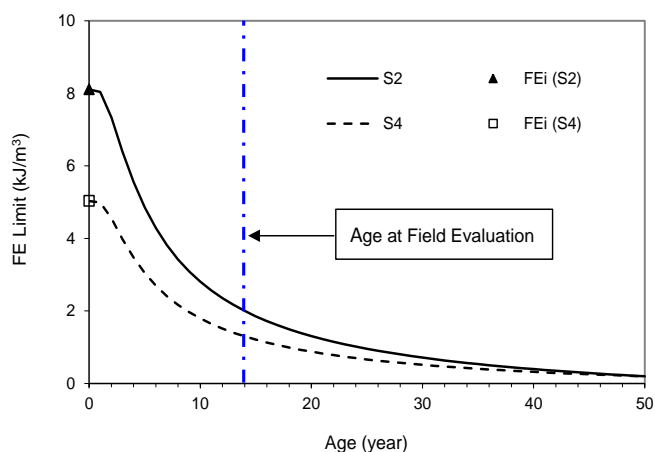


Fig. 5. Predicted FE Limit Aging Curves for Sections 2 and 4 (Assuming $k_1 = 3$).

0.2 kJ/m³ based on field specimens, and t_f was assumed to be 50 years [11].

$$FE_f(t) = FE_i - (FE_i - FE_{min}) \cdot [S_n(t)]^{k_1} \tag{1}$$

As an example, the predicted initial fracture energies and associated FE limit aging curves for Sections 2 and 4 using Eq. (1) are presented in Fig. 5. The FE limits determined on field aged cores (see Fig. 4(a)) and a k_1 value of 3 were used for these predictions. It is expected that a change in k_1 will lead to changes in

both the initial fracture energy and the rate of change of FE limit with aging.

Three steps were employed to determine the aging parameter, including (i) model prediction based on selected k_1 values, (ii) linear regression between predicted and observed cracking performance data for each k_1 , and (iii) determination of optimum k_1 based on regression results. Specifically, eight k_1 values ranging from 0.5 to 5.0 were selected to conduct top-down cracking predictions. For each k_1 , a linear regression was conducted to examine the error between the predicted and observed crack initiation times for all ten sections. It was found that a k_1 value of 3 resulted in the highest R-Square value of 0.933 (Fig. 6), indicating the best match between the predicted and observed crack initiation times.

Predictions Using the Calibrated Model

The final prediction of cracking performance for each section using the calibrated model was presented in terms of a normalized crack amount (CA/CA_{max}) versus time, where CA denotes crack amount and CA_{max} is the maximum crack amount for pavement failure [11]. Fig. 7 shows the predicted cracking performance for Sections 2 and 4. As can be seen, the crack amount increased over time in a stepwise manner for both projects. The moment of the first increase of crack amount (i.e., the first step) corresponds to the onset of cracking, and the slope of the straight line connecting the point for onset of cracking and the point for maximum crack amount represents the overall rate of crack growth. Test sections 2 and 4

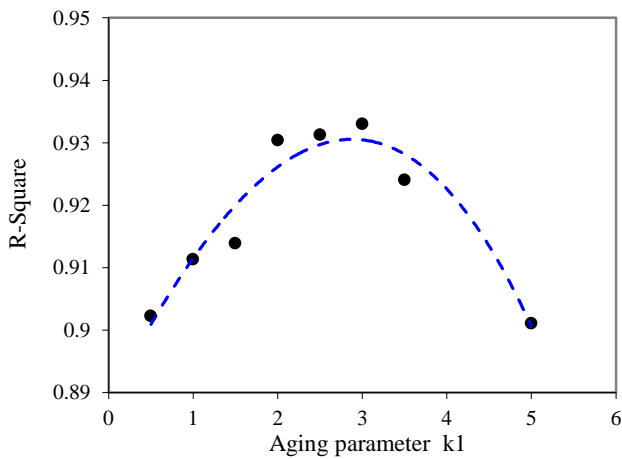


Fig. 6. R-Square Value Determined Based on Linear Regression Results for each k_1 Value.

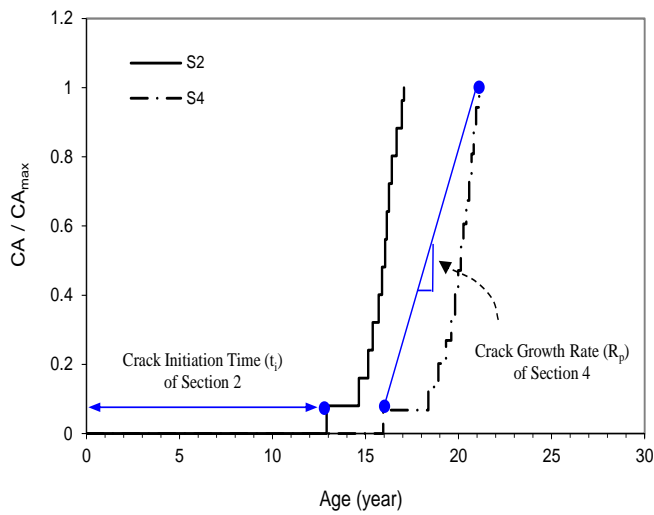


Fig. 7. Predicted Cracking Performance for Sections 2 and 4.

were subjected to very similar traffic condition and the same climatic condition. However, the pavement structure and mixture properties were different. More specifically, Section 2 had a thinner AC layer and a weaker base layer, which resulted in higher tensile stresses and load-induced damage than those of Section 4 for each passing of traffic load. Although the mixture in Section 2 had a higher fracture energy limit (indicating higher tolerance to fracture) than that of Section 4, the overall effect of all key factors led to the worse cracking performance of Section 2, in terms of a shorter time to crack initiation and a faster rate of crack propagation than Section 4.

Fig. 8 presents the predicted crack initiation times for all ten projects. The field observation-based crack initiation times were also shown for comparison purpose. As can be seen, all ten sections were divided into two groups: Group 1 has four sections with all observed crack initiation times less than ten years (Fig. 8(a)), while Group 2 includes six sections with better performance (Fig. 8(b)). Overall, the differences between predicted and observed results are within three years for all but one section. Specifically, the crack initiation time for Section 3 was under-predicted by about five

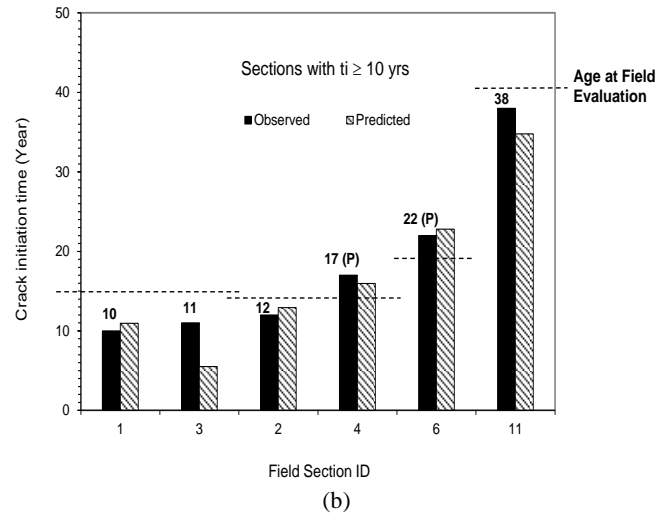
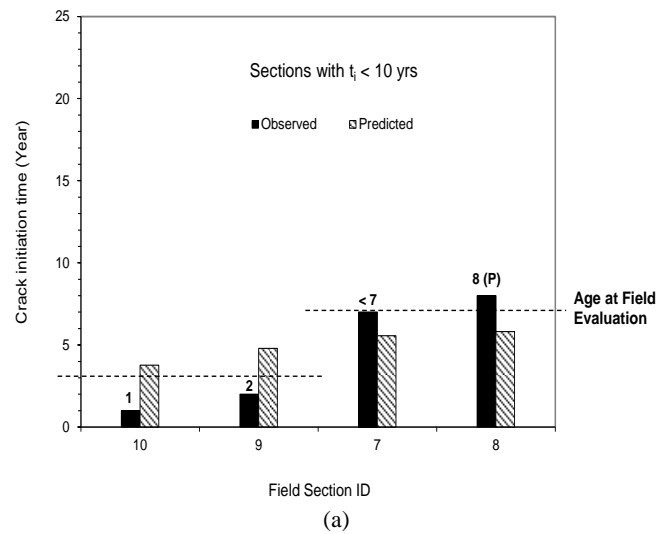


Fig. 8. Predicted vs. Observed Crack Initiation Times for (a) Poor-performing Sections, and (b) Sections with Better Cracking Performance.

years, which were due to the relatively low fracture energy limit in combination with the high traffic volume of this section. It should be noted that healing potential is tied with mixture fracture energy in the current model [11]. In this case, lower healing potential (due to lower fracture energy) allowed faster damage accumulation and cracking in Section 3 when it was subjected to a very high traffic volume. In addition, predicted cracking states were examined as another way to illustrate the accuracy of the model. It appeared that the predicted and observed cracking states at the time of field evaluation were consistent for all six sections in Group 2, while they were not consistent for three out of all four poor-performing sections in Group 1.

The predicted crack growth rate for each field section is presented with its corresponding crack initiation time in Fig. 9. As expected, the crack growth rate and crack initiation time are generally inversely-related. In other words, sections with short crack initiation times exhibited high crack growth rates and vice versa.

Model Validation

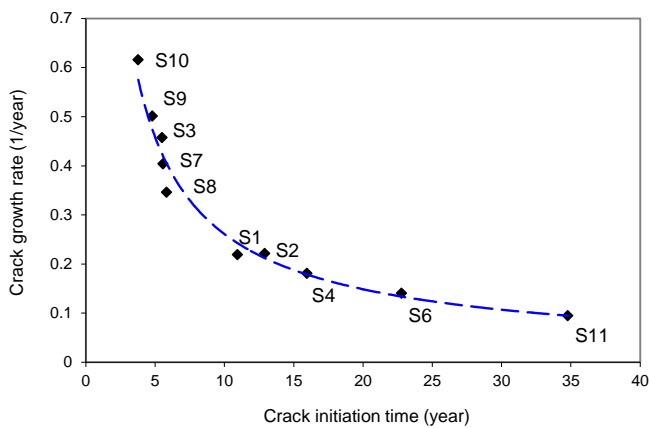


Fig. 9. Predicted Crack Growth Rate Versus Crack Initiation Time.

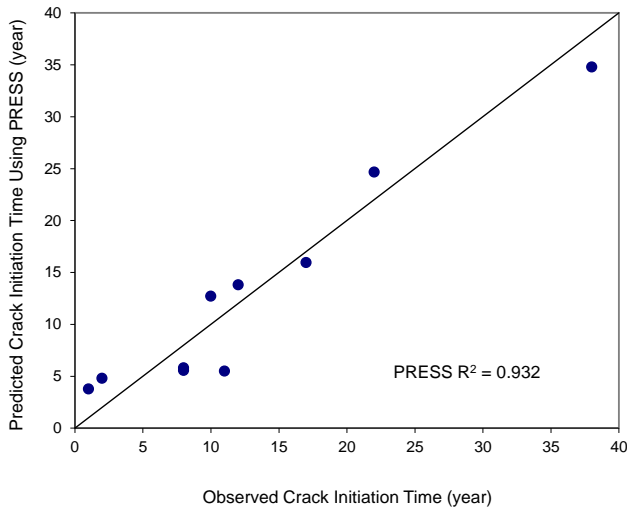


Fig. 10. Predicted Crack Initiation Times Using PRESS Versus Observations.

Validation of the performance model was the final step in the model-development process. Three methods are commonly used in validating a regression model: i) Collection of new data which requires the use of a different data set; ii) Data splitting which requires a large data set that can be divided for use in calibration and validation separately; and iii) The PRESS approach which is typically used to valid regression models based on small size data sets [19]. Since the data set available for this study was small which included only ten test sections, the PRESS method was employed in the validation process. In other words, model validation was conducted using the PRESS procedure based on the same sections as those used for model calibration.

In the PRESS procedure, (n-1) out of all n data sets/sections (here, n = 10) were used at each time to determine the aging parameter k_1 (i.e., a new model was calibrated with nine sections at each time), and then one independent prediction was made for the remaining section using the calibrated model. The model calibration and subsequent independent prediction were conducted ten times following the same procedure. The independent predictions were then compared to the observed crack initiation times to evaluate the

predictability of the model, for which the PRESS R^2 was calculated using the following equation.

$$R^2(PRESS) = 1 - \frac{\left[\sum_{i=1}^n (Y_i - \hat{Y}_i) \right]^2}{\left[\sum_{i=1}^n (Y_i - \bar{Z}_i) \right]^2} \quad (2)$$

Where, Y_i is the observed crack initiation time for Section i, \hat{Y}_i is the independent prediction for Section i, \bar{Z}_i denotes the average of predicted crack initiation times for all sections except for Section i which was excluded for new model calibration.

Fig. 10 presents the comparison between the independent predictions using the PRESS procedure and the observations, where the PRESS R^2 was determined to be 0.932. Clearly, there is a good degree of closeness between the PRESS R^2 and the R^2 of the full model (i.e., the calibrated model using all ten sections), indicating the strong predictive capability of the full model.

Closure

Calibrating and validating an HMA-FM-based enhanced cracking performance model were undertaken using ten selected Florida sections, including determination of crack initiation times based on data from pavement conditioning survey and independent field inspection, determination of calibration factor(s) of the performance model by matching as closely as possible predicted and observed cracking performance, and determination of the predictability of the calibrated model using the PRESS approach. A summary of findings is presented as follows:

- The cracking states of field sections determined based on crack rating data were not always consistent with those obtained from independent field inspection. The final decision was made in favour of the “cracked” state whenever an inconsistency was encountered.
- Four out of the ten field sections had poor cracking performance with crack initiation times less than ten years. These sections were relatively young and had been in-service for less than eight years.
- The aging parameter k_1 was the only calibration factor of the performance model, which was determined to be 3.0 by running a matrix of 8 (number of k_1 -values) by 10 (number of sections) model predictions and by matching as closely as possible predicted and observed crack initiation times.
- Final predictions using the calibrated model showed that the predicted and observed cracking states at the time of field evaluation were consistent for sections with good cracking performance.
- The predicted crack growth rates and crack initiation times were found to be inversely-related. The trend is reasonable and agrees with field experience.
- The model validation effort using the PRESS procedure showed that the calibrated performance model has a strong predictability of top-down cracking performance as indicated by a high value of PRESS R^2 .

In conclusion, the calibration and validation effort using a limited number of Florida sections showed that the HMA-FM-E reasonably represents and accounts for the most significant factors that affect

top-down cracking in the field. Therefore, the model is ready for use in predicting top-down cracking in field sections. Further calibration of the model is recommended when more field sections with more and high quality data are available. Moreover, further development and integration of submodels such as the predictive relationship for initial fracture energy based on gradation characterization and volumetric properties can be included to make the HMA-FM-E a Level-3 design tool suitable for use in the mechanistic-empirical pavement design. In addition, it would be more realistic to use an equivalent daily loading history that has a more representative load spectra and distribution in future model development.

Acknowledgements

The authors would like to express their gratitude to the American Association of State Highway and Transportation Officials and the Federal Highway Administration for providing technical and financial support for this study.

References

- Gerritsen, A. H., Van Gurp, C.A.P.M., Van Der Heide, J.P.J., Molenaar, A.A.A., and Pronk, A.C. (1987). Prediction and Prevention of Surface Cracking in Asphaltic Pavements. *Proceedings of the 6th International Conference on Structural Design of Asphalt Pavements*, Ann Arbor, Michigan, USA, pp. 378-391.
- Matsuno, S. and Nishizawa, T. (1992). Mechanism of Longitudinal Surface Cracking in Asphalt Pavement. *Proceedings of the 7th International Conference on Asphalt Pavements*, University of Nottingham, UK, 2, pp. 277-291.
- Uhlmeyer, J.S., Willoughby, K., Pierce, L.M., and Mahoney, J.P. (2000). Top-down Cracking in Washington State Asphalt Concrete Wearing Courses. *Transportation Research Record*, No. 1730, pp. 110-116.
- Myers, L.A. and Roque, R. (2002). Top-down Crack Propagation in Bituminous Pavements and Implications for Pavement Management. *Journal of the Association of Asphalt Paving Technologists*, 71, pp. 651-670.
- Roque, R., Zhang, Z., and Sankar, B. (1999). Determination of Crack Growth Rate Parameters of Asphalt Mixtures Using the SuperPave Indirect Tensile Test (IDT). *Journal of the Association of Asphalt Paving Technologists*, 68, pp. 404-433.
- Baek, C., Underwood, B. S., and Kim, Y.R. (2012). Effects of Oxidative Aging on Asphalt Mixture Properties. *Transportation Research Record*, No. 2296, pp. 77-85.
- Myers, L.A., Roque, R., and Ruth, B.E. (1998). Mechanisms of Surface Initiated Longitudinal Wheel Path Cracks in High-type Bituminous Pavements. *Journal of the Association of Asphalt Paving Technologists*, 67, pp. 402-432.
- Wang, L.B., Myers, L.A., Mohammad, L.N., and Fu, Y.R. (2003). Micromechanics Study on Top-Down Cracking. *Transportation Research Record*, No. 1853, pp. 121-133.
- Zhang, Z., Roque, R., Birgisson, B., and Sangpetngam, B. (2001). Identification and Verification of a Suitable Crack Growth Law. *Journal of the Association of Asphalt Paving Technologists*, 70, pp. 206-241.
- Roque, R., Birgisson, B., Sangpetngam, B., and Zhang, Z. (2002). Hot Mix Asphalt Fracture Mechanics: A Fundamental Crack Growth Law for Asphalt mixtures. *Journal of the Association of Asphalt Paving Technologists*, 71, pp. 816-827.
- Roque, R., Zou, J., Kim, Y.R., Beak, C., Thirunavukkarasu, S., Underwood, B. S., and Guddati, M.N. (2010). *Top-down Cracking of HMA Layers: Models for Initiation and Propagation*, NCHRP Web-Only Document 162, National Cooperative Highway Research Program, Transportation Research Board of the National Academies. (URL: onlinepubs.trb.org/onlinepubs/nchrp/nchrp_w162.pdf, last accessed on 09/2013.)
- Zou, J. and Roque, R. (2011). Top-Down Cracking: Enhanced Performance Model and Improved Understanding of Mechanisms. *Journal of the Association of Asphalt Paving Technologists*, 80, pp. 255-287.
- Zou, J., Roque, R., and Byron, T. (2012). Effect of HMA Aging and Potential Healing on Top-Down Cracking Using HVS. *International Journal of Road Materials and Pavement Design*, 13(3), pp. 518-533.
- Florida Department of Transportation (2009). *Flexible Pavement Condition Survey Handbook*, Tallahassee, FL, USA.
- Roque, R., Birgisson, B., Drakos, C., Sedwick, S., Garcia, O., Jajliardo, A., and Kim, J. (2006). *Evaluation of Surface-Initiated Longitudinal Wheel Path Cracking (II): Effect of Asphalt Mixture Properties and Characteristics*, Final Report of Florida Department of Transportation, University of Florida, Gainesville, Florida, USA.
- Roque, R., Buttlar, W.G., Ruth, B.E., Tia, M., Dickson, S.W., and Reid, B. (1997). *Evaluation of SHRP Indirect Tension Tester to Mitigate Cracking in Asphalt Pavements and Overlays*, Final Report of Florida Department of Transportation, University of Florida, Gainesville, Florida, USA.
- Buttlar, W.G., Roque, R., and Reid, B. (1998). Automated Procedure for Generation of Creep Compliance Master Curve for Asphalt Mixtures. *Transportation Research Record*, No. 1630, pp. 28-36.
- Larson, G. and Dempsey, B. (2003). *Enhanced Integrated Climatic Model: User's Guide Version 3.0*, Applied Research Associates, ERES Division, Champaign, Illinois, USA.
- Lytton, R.L., Uzan, J., Fernando, E.G., Roque, R., Hiltunen, D., and Stoffels, S.M. (1993). *Development and Validation of Performance Prediction Models and Specifications for Asphalt Binders and Paving Mixes*. SHRP-A-357, Strategic Highway Research Program, National Research Council, Washington, DC, USA.